

Measurements of F_2 and $xF_3^\nu - xF_3^{\bar{\nu}}$ from CCFR ν_μ -Fe and $\bar{\nu}_\mu$ -Fe Data in a Physics Model-Independent Way

U. K. Yang,⁷ T. Adams,⁴ A. Alton,⁴ C. G. Arroyo,² S. Avvakumov,⁷ L. de Barbaro,⁵ P. de Barbaro,⁷ A. O. Bazarko,² R. H. Bernstein,³ A. Bodek,⁷ T. Bolton,⁴ J. Brau,⁶ D. Buchholz,⁵ H. Budd,⁷ L. Bugel,³ J. Conrad,² R. B. Drucker,⁶ B. T. Fleming,² J. A. Formaggio,² R. Frey,⁶ J. Goldman,⁴ M. Goncharov,⁴ D. A. Harris,⁷ R. A. Johnson,¹ J. H. Kim,² B. J. King,² T. Kinnel,⁸ S. Koutsoliotas,² M. J. Lamm,³ W. Marsh,³ D. Mason,⁶ K. S. McFarland,⁷ C. McNulty,² S. R. Mishra,² D. Naples,⁴ P. Nienaber,³ A. Romosan,² W. K. Sakumoto,⁷ H. Schellman,⁵ F. J. Sciulli,² W. G. Seligman,² M. H. Shaevitz,² W. H. Smith,⁸ P. Spentzouris,² E. G. Stern,² N. Suwonjandee,¹ A. Vaitaitis,² M. Vakili,¹ J. Yu,³ G. P. Zeller,⁵ and E. D. Zimmerman²

(CCFR/NuTeV Collaboration)

¹University of Cincinnati, Cincinnati, Ohio 45221

²Columbia University, New York, New York 10027

³Fermi National Accelerator Laboratory, Batavia, Illinois 60510

⁴Kansas State University, Manhattan, Kansas 66506

⁵Northwestern University, Evanston, Illinois 60208

⁶University of Oregon, Eugene, Oregon 97403

⁷University of Rochester, Rochester, New York 14627

⁸University of Wisconsin, Madison, Wisconsin 53706

(Received 15 September 2000)

We report on the extraction of the structure functions F_2 and $\Delta xF_3 = xF_3^\nu - xF_3^{\bar{\nu}}$ from CCFR ν_μ -Fe and $\bar{\nu}_\mu$ -Fe differential cross sections. The extraction is performed in a physics model-independent (PMI) way. This first measurement of ΔxF_3 , which is useful in testing models of heavy charm production, is higher than current theoretical predictions. The ratio of the F_2 (PMI) values measured in ν_μ and μ scattering is in agreement (within 5%) with the predictions of next-to-leading-order parton distribution functions using massive charm production schemes, thus resolving the long-standing discrepancy between the two sets of data.

DOI: 10.1103/PhysRevLett.86.2742

PACS numbers: 12.38.Qk, 13.15.+g, 24.85.+p, 25.30.Pt

Deep inelastic lepton-nucleon scattering experiments have been used to determine the quark distributions in the nucleon. However, the quark distributions determined from muon [1] and neutrino [2] experiments were found to be different at small values of Bjorken x , because of a disagreement in the extracted structure functions. In this Letter, we report on a measurement of differential cross sections and structure functions from CCFR ν_μ -Fe and $\bar{\nu}_\mu$ -Fe data. The neutrino-muon difference is resolved by extracting the ν_μ structure functions in a physics model independent (PMI) way. We also report on the first measurement of $\Delta xF_3 = xF_3^\nu - xF_3^{\bar{\nu}}$, which is used to test models of heavy charm production.

The sum of ν_μ and $\bar{\nu}_\mu$ differential cross sections for charged current interactions on an isoscalar target is related to the structure functions as follows:

$$F(\epsilon) \equiv \left[\frac{d^2\sigma^\nu}{dx dy} + \frac{d^2\sigma^{\bar{\nu}}}{dx dy} \right] \frac{(1-\epsilon)\pi}{y^2 G_F^2 M E_\nu} \\ = 2xF_1[1 + \epsilon R] + \frac{y(1-y/2)}{1+(1-y)^2} \Delta xF_3. \quad (1)$$

Here G_F is the Fermi weak coupling constant, M is the nucleon mass, E_ν is the incident neutrino energy, the scaling variable $y = E_h/E_\nu$ is the fractional energy trans-

ferred to the hadronic vertex, E_h is the final state hadronic energy, and $\epsilon \approx 2(1-y)/[1+(1-y)^2]$ is the polarization of the virtual W boson. The structure function $2xF_1$ is expressed in terms of F_2 by $2xF_1(x, Q^2) = F_2(x, Q^2) \times \frac{1+4M^2x^2/Q^2}{1+R(x, Q^2)}$, where Q^2 is the square of the four-momentum transfer to the nucleon, $x = Q^2/2ME_h$ (the Bjorken scaling variable) is the fractional momentum carried by the struck quark, and $R = \frac{\sigma_L}{\sigma_T}$ is the ratio of the cross sections of longitudinally to transversely polarized W bosons.

A similar equation for the case of muon scattering relates the cross sections to the structure functions. However, there are significant differences originating from the scattering on strange (s) and charm (c) quarks. The ΔxF_3 term, which in leading order $\approx 4x(s-c)$, is not present in the μ scattering case. In addition, in a charged current ν_μ interaction involving s (or \bar{c}) quarks, there is a threshold suppression originating from the production of heavy c quarks in the final state. For μ scattering, while there is no suppression for scattering from s quarks, there is larger suppression when scattering from c quarks since there are two heavy quarks (c and \bar{c}) in the final state.

In previous analyses [2] of ν_μ data, light flavor universal physics model-dependent (PMD) structure functions

were extracted by applying a slow rescaling correction to correct for the charm mass suppression in the final state. In addition, the ΔxF_3 term (used as input in the extraction) was calculated from a leading order charm production model. Recent calculations [3–5] indicate that there are large theoretical uncertainties in the charm production modeling for both ΔxF_3 and the slow rescaling corrections. Therefore, in the new analysis reported here, slow rescaling corrections are not applied, and ΔxF_3 and F_2 are extracted from two-parameter fits to the data. We compare the values of ΔxF_3 to various charm production models. The extracted PMI values for F_2^ν are then compared with F_2^μ within the framework of next-to-leading-order (NLO) models for charm production.

The CCFR experiment collected data using the Fermilab Tevatron Quad-Triplet wide-band ν_μ and $\bar{\nu}_\mu$ beam. The CCFR detector [6] consists of a steel-scintillator target calorimeter instrumented with drift chambers, followed by a toroidally magnetized muon spectrometer. The hadron energy resolution is $\Delta E_h/E_h = 0.85/\sqrt{E_h}$ (GeV), and the muon momentum resolution is $\Delta p_\mu/p_\mu = 0.11$. By measuring the hadronic energy (E_h), muon momentum (p_μ), and muon angle (θ_μ), we construct three independent kinematic variables x , Q^2 , and y . The relative flux at different energies, obtained from the events with low hadron energy ($E_h < 20$ GeV), is normalized so that the neutrino total cross section equals the world average $\sigma^{\nu N}/E = (0.677 \pm 0.014) \times 10^{-38}$ cm²/GeV and $\sigma^{\bar{\nu}N}/\sigma^{\nu N} = 0.499 \pm 0.005$ [2]. After fiducial and kinematic cuts ($p_\mu > 15$ GeV, $\theta_\mu < 0.150$, $E_h > 10$ GeV, and $30 < E_\nu < 360$ GeV), the data sample consists of 1 030 000 ν_μ and 179 000 $\bar{\nu}_\mu$ events. Dimuon events are removed because of the ambiguous identification of the leading muon for high- y events.

The raw differential cross sections per nucleon on iron are determined in bins of x , y , and E_ν ($0.01 < x < 0.65$, $0.05 < y < 0.95$, and $30 < E_\nu < 360$ GeV). Figure 1 shows typical differential cross sections at $E_\nu = 150$ GeV (complete tables are available [7]). For all energies, the cross sections are in good agreement with NLO parton distribution functions (PDFs) (with massive charm production schemes, e.g., MRST99 [8] or CTEQ4HQ [9]). The dashed lines show the predictions from the Thorne and Roberts variable flavor scheme (TR-VFS) [4] QCD calculation using MRST99 extended [10] PDFs. This calculation includes an improved treatment of massive charm production. The QCD predictions, which are on free neutrons and protons, are corrected for nuclear [2], higher twist [11,12], and radiative effects [13]. Also shown are the predictions from a CCFR leading order (LO) QCD inspired fit used for calculation of acceptance and resolution smearing corrections. As expected from QCD, the CCFR cross section data exhibit a quadratic y dependence at small x for ν_μ and $\bar{\nu}_\mu$, and a flat y distribution at high x for ν_μ .

Next, the raw cross sections are corrected for electroweak radiative effects [13], the W boson propagator, and for the 5.67% nonisoscalar excess of neutrons over

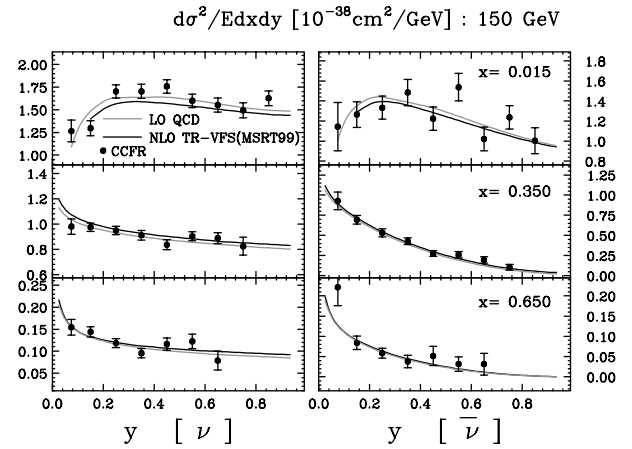


FIG. 1. Typical raw differential cross sections at $E_\nu = 150$ GeV (both statistical and systematic errors are included). The CCFR data are in good agreement with the NLO TR-VFS QCD calculation using MRST99 PDFs (dashed line). The solid line is a CCFR LO QCD inspired fit.

protons in iron (only important at high x). Values of ΔxF_3 and F_2 are extracted from the sums of the corrected ν_μ -Fe and $\bar{\nu}_\mu$ -Fe differential cross sections according to Eq. (1). However, it is challenging to fit ΔxF_3 , R , and $2xF_1$ using the y distribution at a given x and Q^2 because of the strong correlation between the ΔxF_3 and R terms, unless the full range of y is covered by the data. Covering this range (especially the high y region) is difficult because of the low acceptance. Therefore, we restrict the analysis to two-parameter fits.

Our strategy is to fit ΔxF_3 and F_2 (or equivalently $2xF_1$) for $x < 0.1$ where the ΔxF_3 contribution is relatively large, while constraining R using the $R_{\text{world}}^{\mu/e}$ [14] QCD-inspired empirical fit to all available electron and muon scattering data. The $R_{\text{world}}^{\mu/e}$ fit is also in good agreement with NMC R^μ data [1] at low x , and with the most recent theoretical prediction [12] for R [a next-to-NLO (NNLO) QCD calculation including target mass effects]. For $x < 0.1$, R in neutrino scattering is expected to be somewhat larger than R for muon scattering because of the production of massive charm quarks in the final state. A correction for this difference is applied to $R_{\text{world}}^{\mu/e}$ using a leading order slow rescaling model to obtain an effective R for neutrino scattering, R_{eff}^ν . The difference between $R_{\text{world}}^{\mu/e}$ and R_{eff}^ν is used as a systematic error. Because of the positive correlation between R and ΔxF_3 , the extracted values of F_2 are rather insensitive to the input R . In contrast, the extracted values of ΔxF_3 are sensitive to the assumed value of R , which is reflected in a larger systematic error. The values of ΔxF_3 are sensitive to the energy dependence of the neutrino flux ($\sim y$ dependence), but are insensitive to the absolute normalization. The uncertainty on the flux shape is estimated by using the constraint that F_2 and xF_3 should be flat over y (or E_ν) for each x and Q^2 bin.

Because of the limited statistics, we use large bins in Q^2 in the extraction of ΔxF_3 with bin centering corrections applied using the NLO TR-VFS calculation [4] with the MRST99 PDFs. Figure 2 (left) shows the extracted values of ΔxF_3 as a function of x , including both statistical and systematic errors, compared to various theoretical methods for modeling heavy charm production within a QCD framework. The three-flavor fixed flavor scheme (FFS) [15] assumes that there is no intrinsic charm in the nucleon, and that all scattering from c quarks occurs via the gluon-fusion diagram. The concept behind the VFS proposed by Aivazis, Collins, Olness, and Tung (ACOT) [5,16] is that at low scale, μ , one uses the three-flavor FFS scheme, while above some scale, an intrinsic charm sea (which is evolved from zero) is introduced. The concept of the TR-VFS scheme [4] is similar, except that at intermediate scale it interpolates smoothly between the two regions. Both the FFS and VFS schemes have been implemented by Kramer, Lampe, and Spiesberger (KLS) [3], ACOT, and Kretzer and Schienbein [17]. The last two implementations agree with each other, but not with KLS (there was a mistake in the KLS calculation) [18].

Shown are the predictions from the TR-VFS scheme (implemented with MRST99 PDFs and the suggested scale $\mu = Q$) and along with the predictions from two other NLO calculations, ACOT-VFS [implemented with CTEQ4HQ PDFs and their recent suggested scale $\mu = m_c$ for $Q < m_c$, and $\mu^2 = m_c^2 + 0.5Q^2(1 - m_c^2/Q^2)^n$ for $Q > m_c$ with $n = 2$ [5]] and the FFS (implemented with the GRV94 [19] PDFs and their recommended scale

$\mu = 2m_c$). Also shown are the predictions from the leading order QCD fit to the CCFR dimuon [20] data.

Figure 2 (right) shows the sensitivity to the choice of scale. For example, the data do not favor the choice of scale, $\mu = 2Pt_{\max}$ in the ACOT-VFS calculation with CTEQ4HQ PDFs. This high scale (originally suggested by ACOT and used in the CCFR dimuon analysis [20]) implies that the calculation is in the four-flavor region even at $x = 0.015$ and $Q^2 = 1.0 \text{ GeV}^2$ (and yields a large negative result). With reasonable choices of scale, all the theoretical models yield similar results. However, at low Q^2 , our ΔxF_3 data are higher than all of the theoretical models. The difference between data and theory may be due to an underestimate of the strange sea at low Q^2 , or from missing NNLO terms. The question of the strange sea would be addressed by a global NLO analysis which combines the neutrino data for dimuons, ΔxF_3 and F_2^ν , with $F_2^{\mu,e}$.

As discussed above, values of F_2 for $x < 0.1$ are extracted from two-parameter fits to the y distributions. In the $x > 0.1$ region, the contribution from ΔxF_3 is small and the extracted values of F_2 are insensitive to ΔxF_3 . Therefore, we extract values of F_2 with an input value of R and with ΔxF_3 constrained to the TR-VFS (MRST99) predictions. Figure 3 shows the ratio of our F_2^ν (PMI) measurements divided by $(18/5)F_2^\mu$ (NMC [1] or BCDMS [21]) or $(18/5)F_2^e$ (SLAC [22]) measurements [23]. The overall normalization errors of 2% (CCFR),

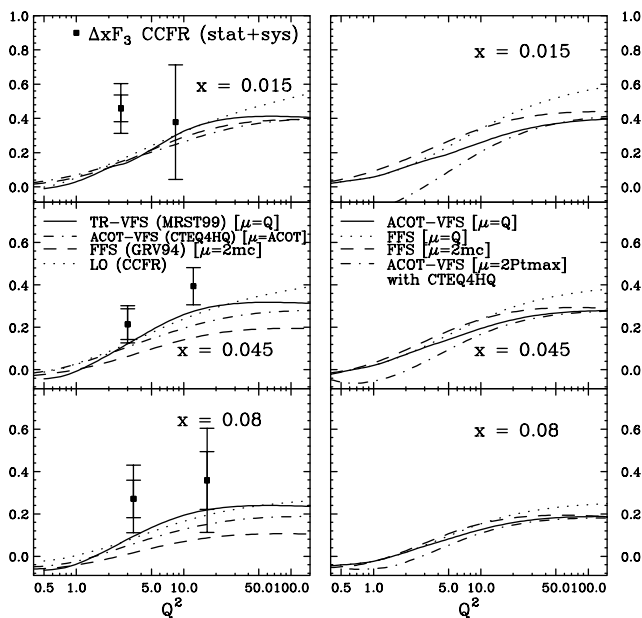


FIG. 2. ΔxF_3 data as a function of x compared with various schemes for massive charm production: (left) TR-VFS (MRST99), ACOT-VFS (CTEQ4HQ), FFS (GRV94), and the CCFR-LO (a leading order model with a slow rescaling correction); (right) sensitivity of the theoretical calculations to the choice of scale.

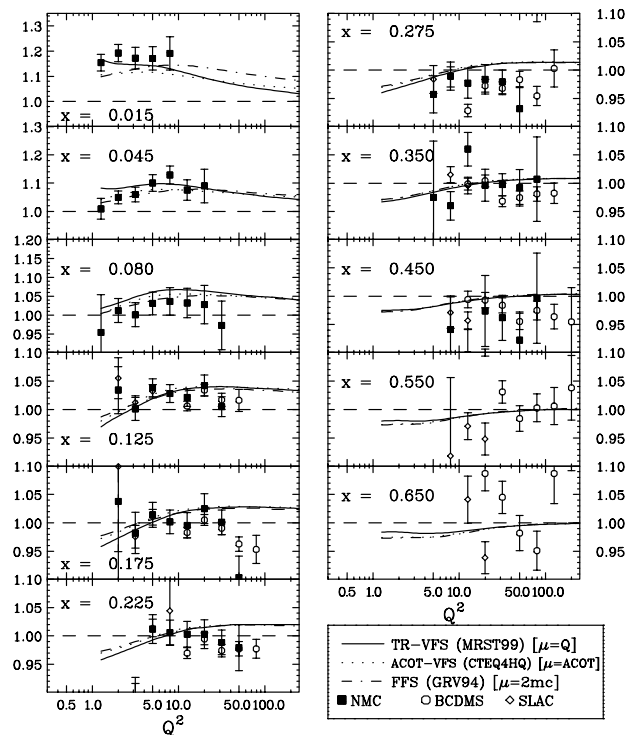


FIG. 3. The ratio of F_2^ν (PMI) data divided by F_2^μ (NMC or BCDMS) or F_2^e (SLAC). Both statistical and systematic errors are included. Also shown are the predictions of the TR-VFS (MRST99), ACOT-VFS (CTEQ4HQ), and FFS (GRV94) heavy flavor calculations.

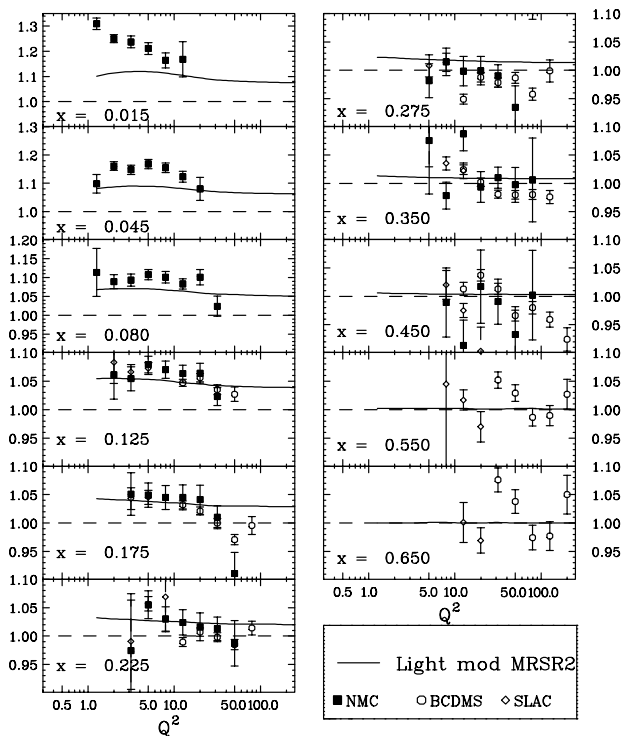


FIG. 4. The ratio of the previous F_2^ν (PMD) data divided by $(18/5)F_2^\mu$ (NMC or BCDMS) or $(18/5)F_2^e$ (SLAC). Shown are the predictions of the MRSR2 light-flavor PDFs (the curves with CTEQ4M are very similar).

and 2.5% (NMC) are not shown. Within 5%, the ratio is in agreement with the predictions of the TR-VFS (MRST99), ACOT-VFS (CTEQ4HQ), and FFS (GRV94) calculations [24].

In the calculation of the theoretical predictions, we have also included corrections for nuclear effects [2]. As mentioned earlier, the extracted values of F_2 from the two-parameter fits are insensitive to R . For example, if we perform simultaneous two-parameter fits to F_2 and R [while keeping ΔxF_3 fixed to the TR-VFS (MRST99) values], the extracted R values at $x = 0.01$ are smaller than R_{eff}^ν , but F_2 changes by only 2%–3%.

In the previous analysis [2] of the CCFR data, the ratio of extracted values of F_2^ν (PMD) data divided by $(18/5)F_2^\mu$ (NMC) at the lowest $x = 0.015$ and Q^2 bin were 20% higher than the predictions of the light-flavor PDFs such as MRSR2 [25] or CTEQ4M [9] (see Fig. 4). About 10% of the difference originates from having used a leading order model for ΔxF_3 versus using our new measurement. Another 6% originates from having used the leading order slow rescaling corrections, instead of using NLO massive charm production models. The remaining 3% originates from improved modeling of the low Q^2 PDFs (which changes the radiative corrections and the overall absolute normalization to the total neutrino cross sections). For higher Q^2 at $x = 0.015$, and for the next two x bins ($x = 0.045$ and 0.08), the smaller difference

between the PMI and PMD results is due to equal contributions from the ΔxF_3 and the difference in the slow rescaling corrections. For the higher x bins ($x > 0.1$), the contribution of ΔxF_3 is small, and the slow rescaling corrections in the leading order model are the same as those with the NLO theories. Therefore, the NMC and CCFR data are in agreement at large x whether PMI or PMD structure functions are used in the comparison.

In conclusion, the ratio of F_2 (PMI) values measured in neutrino-iron and muon-deuterium scattering are in agreement with the predictions of next-to-leading-order PDFs (using massive charm production schemes), thus resolving the long-standing discrepancy between the two sets of data. The first measurement of ΔxF_3 is higher than current theoretical predictions.

- [1] M. Arneodo *et al.*, Nucl. Phys. **B483**, 3 (1997).
- [2] W.G. Seligman *et al.*, Phys. Rev. Lett. **79**, 1213 (1997).
- [3] G. Kramer, B. Lampe, and H. Spiesberger, Z. Phys. C **72**, 99 (1996).
- [4] R.S. Thorne and R.G. Roberts, Phys. Lett. B **421**, 303 (1998); Rutherford Appleton Laboratory Report No. RAL-TR-2000-048, 2000.
- [5] M. Aivazis, J. Collins, F. Olness, and W.K. Tung, Phys. Rev. D **50**, 3102 (1994).
- [6] W.K. Sakumoto *et al.*, Nucl. Instrum. Methods Phys. Res., Sect. A **294**, 179 (1991); B. King *et al.*, *ibid.* **302**, 254 (1991).
- [7] <http://www-e815.fnal.gov/~ukyung>; U.K. Yang, Ph.D. thesis, University of Rochester [UR-1583, 2000].
- [8] A.D. Martin *et al.*, Eur. Phys. J. C **14**, 133 (2000).
- [9] H.L. Lai *et al.*, Z. Phys. C **74**, 463 (1997).
- [10] For $Q^2 < 1.2 \text{ GeV}^2$, the MRST PDFs are extended according to the Q^2 dependence of GRV94 PDFs.
- [11] U.K. Yang and A. Bodek, Phys. Rev. Lett. **82**, 2467 (1999).
- [12] U.K. Yang and A. Bodek, Eur. Phys. J. C **13**, 241 (2000).
- [13] D. Yu. Bardin and V.A. Dokuchaeva, Joint Institute of Research Institute Report No. JINR-E2-86-260, 1986.
- [14] L.W. Whitlow *et al.*, Phys. Lett. B **250**, 193 (1990).
- [15] E. Laenen *et al.*, Nucl. Phys. **B392**, 162 (1993).
- [16] M. Aivazis, F. Olness, and W.K. Tung, Phys. Rev. Lett. **65**, 2339 (1990).
- [17] S. Kretzer and I. Schienbein, Phys. Rev. D **58**, 094035 (1998).
- [18] F. Olness and S. Kretzer (private communication).
- [19] M. Gluck *et al.*, Z. Phys. C **67**, 433 (1995).
- [20] A. Bazarko *et al.*, Z. Phys. C **65**, 189 (1995).
- [21] A.C. Benvenuti *et al.*, Phys. Lett. B **237**, 592 (1990).
- [22] L.W. Whitlow *et al.*, Phys. Lett. B **282**, 475 (1992).
- [23] An empirical fit [1] to the SLAC, BCDMS, NMC F_2^d data is used for bin-center correction to these data.
- [24] Correction for the difference between ν -Fe and μ -Fe nuclear effects would make the agreement better [C. Boros *et al.*, Phys. Lett. B **468**, 161 (1999)]. Also, the predictions would increase by $\approx 5\%$ at $x = 0.015$, if a strange sea which describes the ΔxF_3 data is used.
- [25] A.D. Martin *et al.*, Phys. Lett. B **387**, 419 (1996).